International Journal of Mechanical Sciences 63 (2012) 1–11

Contents lists available at SciVerse ScienceDirect

International Journal of Mechanical Sciences

journal homepage: www.elsevier.com/locate/ijmecsci

Analytical modeling and experimental investigation of ultrasonic-vibration assisted oblique turning, part I: Kinematics analysis

M.J. Nategh [a,*], H. Razavi [a], A. Abdullah [b]

[a] Tarbiat Modares University, Mechanical Engineering Department, Tehran, P.O. Box 14115-143, Iran
[b] Amirkabir University of Technology, Mechanical Engineering Department, Tehran, Iran

ARTICLE INFO

Article history:
Received 3 January 2012
Received in revised form
16 April 2012
Accepted 27 April 2012
Available online 14 May 2012

Keywords:
Ultrasonic vibration
Vibration cutting
Oblique turning
Kinematics
Critical speed

ABSTRACT

The purpose of the present study is the kinematics, dynamics and experimental investigation of ultrasonic-vibration assisted oblique turning. The results are presented in three parts. In the first part, the kinematics of the relative motion between the cutting tool and the work-piece is concerned. The vibration cutting is an intermittent process and cutting in this process is physically implemented in part of the vibration cycle. The critical cutting speed and the cutting duration in vibration oblique turning are other important kinematics factors which are dealt with in this part. For this purpose, three different models have been developed and examined by different case studies.

1. Introduction

In ultrasonic-vibration assisted turning (UAT), the cutting tool vibrates at an ultrasonic frequency along the cutting, feed or radial direction. The vibration is superimposed on the common cutting motion. Applying the vibration in cutting direction (one dimensional UAT) or in cutting and feed directions (elliptical UAT) has gained more popularity because the resulting motion of cutting tool is more effective. The vibration cutting has several advantages such as reduction in the average cutting force, improvement of the surface quality of the machined work-piece, increase in tool life, etc. In the literature, the reduction of the average cutting force as a major advantage of UAT has been attributed to the alternate tool-workpiece engagement and disengagement. Chunxiang et al [1] have discussed about the separation of the tool rake face from chip and the separation of the tool flank from the work-piece. The separation of tool from chip and from work-piece in elliptical vibration has also been clearly mentioned [2–4]. In 1D –UAT, it is also believed that the cutting tool periodically separates from the work-piece [5–10], from the chip [11–19] or from both the work-piece and chip [20,21].

In UAT because of the feed motion, the cutting tool never disengages from work-piece when the process is going on, but instead disengages from the shear zone in machining part of each vibration cycle causing interrupted cutting. This was overlooked in previous researches in spite of its importance in the kinematics analysis of the tool movement relative to the work-piece. It should be mentioned that two different surfaces are actually produced in a turning operation: the main surface of the work-piece remaining after the machining operation; and the lateral surface which is shaped during each revolution of the work-piece and subsequently removed in the form of chip in the next revolution of the work-piece. Non-separating tool-workpiece mechanism causes some regions of the lateral surface to be pressed by the cutting tool edge resulting in an increase of surface hardness in these regions. Therefore, the measurement of the surface hardness can provide a means for verifying this mechanism.

The hardness of the main surface after machining has already been studied [11,14–16]. In these studies, it was observed that surface hardness in one-dimensional UAT with cutting tool vibrating in cutting direction was about 60 less than its value in conventional turning (CT) and was considerably close to the hardness of untreated material. On the other hand, the cutting forces in UAT were about 30 of those in CT; thus the smaller cutting forces made a less intrusive process from UAT. This led to a softer layer compared with CT. Sasahara [22] has studied the effect of different parameters such as tool nose radius, cutting edge shape (sharp or chamfered) and feed rate on the hardness of lateral machined surface in CT. The hardness of the lateral surface has not yet been studied in UAT.

* Corresponding author. Tel.: +98 21 82884396.
E-mail address: nategh@modares.ac.ir (M.J. Nategh).

0020-7403/$ - see front matter © 2012 Elsevier Ltd. All rights reserved.
http://dx.doi.org/10.1016/j.ijmecsci.2012.04.007

Nomenclature

a	vibration amplitude along the cutting velocity (μm)
A,B,b',C,D,H,P	constants
A_S	shear plane area (mm^2)
b	depth of cut (mm)
d	workpiece diameter (mm)
D_j	depth of pressed zone (mm)
f	vibration frequency (Hz)
i	inclination angle (deg.)
K_r	tool cutting edge angle (deg.)
N	spindle rotational speed (rev/min)
P_n	cutting edge normal plane
P_V	velocity plane
t	time (s)
t_{11}	machining interruption instant in the first cycle of vibration (s)
t_{12}	the instant of maximum distance of the cutting tool from the shear zone in the first vibration cycle (s)
t_{13}	machining restart instant in the first cycle of vibration (s)
$t_{n\,1}$	machining interruption instant in the nth cycle of vibration (s)
$t_{n\,2}$	the instant of maximum distance of the cutting tool from the shear zone in the nth vibration cycle (s)
$t_{n\,3}$	machining restart instant in the nth cycle of vibration (s)
V_C	cutting speed (m/s)
V_{cr}	critical cutting speed (m/s)
V_f	feed rate (m/s) or (mm/rev)
$V_{X\,W/T}(t)$	workpiece's velocity component relative to tool in radial direction (m/s)
$V_{Y\,W/T}(t)$	workpiece's velocity component relative to tool in tangential direction (m/s)
$V_{Z\,W/T}(t)$	workpiece's velocity component relative to tool in axial direction (m/s)
$V_{X''\,W/T}(t)$	workpiece's velocity component relative to tool in cutting tool edge direction ($x''y''z''$ coordinate system) (m/s)
$V_{Y''\,W/T}(t)$	workpiece's velocity component relative to tool normal to cutting tool edge in lateral machined surface ($x''y''z''$ coordinate system) (m/s)
$V_{Z''\,W/T}(t)$	workpiece's velocity component relative to tool in z'' direction (or normal to cutting tool edge and also normal to lateral machined surface ($x''y''z''$ coordinate system) (m/s)
$V_{resultant}$	resultant velocity (resultant of cutting speed V_C and feed rate V_f) (m/s)
$\vec{V}_T$	cutting tool's velocity vector in UAT (m/s)
$\vec{V}_W$	workpiece's velocity vector in UAT (with the same magnitude as cutting speed) (m/s)
$\vec{V}_{W/T}$	workpiece's velocity vector relative to tool in UAT (m/s)
$V_\perp$	normal velocity (*first criterion*: y'' component of workpiece's velocity relative to cutting tool, *second criterion*: workpiece's velocity relative to cutting tool in direction perpendicular to the tool rake face, *third criterion*: workpiece's velocity relative to cutting tool in direction normal to shear plane (m/s)
W_j	width of pressed zone (mm)
$x\ y\ z$	machine tool coordinate system: x radial (or depth of cut) direction, y tangential (or cutting velocity) direction and z axial (or negative feed) direction
$x'\ y'\ z'$	intermediate coordinate system (rotated $x\ y\ z$ system by angle $90-K_r$)
$x''\ y''z''$	oblique coordinate system (rotated $x'\ y'\ z'$ system by angle i); x''along the tool's cutting edge, y'' placed on the lateral surface and z''normal to the lateral surface
$X''_{W/T}(t)$	workpiece's position relative to tool in cutting tool edge direction
$Y''_{W/T}(t)$	workpiece's position relative to tool in lateral surface and perpendicular to tool cutting edge (mm)
$Z''_{W/T}(t)$	workpiece's position relative to tool perpendicular to tool cutting edge and normal to lateral surface (mm)
γ_n	normal rake angle (deg.)
Δt_1	noncutting duration in one cycle of vibration
Δt_2	cutting duration in one cycle of vibration
Δt_{total}	vibration cycle time
ϕ_n	normal shear angle (measured in normal plane) (deg.)
ω	angular velocity (rad/s)

In the present study, the kinematics of the tool-workpiece's relative movement in UAT has first been investigated in order to provide real insights in to the underlying mechanism.

The advantages of the vibration assisted cutting lessen as the cutting speed approaches a critical value and virtually disappear when this critical value is exceeded. The critical cutting speed in orthogonal UAT is obtained by $V_{cr}=2\pi a f$, where a and f denote the vibration amplitude and frequency, respectively [1–20, 23–25]. It is more complicated in oblique UAT and needs to be investigated. In addition, the development of a thorough kinematics model requires that the tool engagement and disengagement instants in each cycle of vibration to be specified. This is also a prerequisite for the dynamics analysis of the oblique UAT. In the present study, three different criteria have been introduced to explain the tool engagement/disengagement model. The relations estimating the critical cutting speed and the tool engagement and disengagement instants were subsequently derived. The results were compared through different case studies. The influence of variations in the oblique UAT parameters including the frequency and amplitude of vibration, the cutting tool rake angle, inclination angle, tool cutting edge angle and feed rate on the critical speed and the start and end instants of cutting operation in each cycle of vibration has also been studied. The experimental results of the present study would be presented in Part III.

2. Mechanics of oblique turning

The oblique turning operation is schematically illustrated in Fig. 1. The two lateral and main surfaces are shown in this figure. In this figure i and K_r denote the inclination angle and cutting edge angle, respectively. As is clear from this figure, three coordinate systems have been defined: $x\ y\ z$ coordinate system corresponds to the general coordinate system of CNC lathes; $x'\ y'\ z'$ or intermediate coordinate system is obtained when $x\ y\ z$ coordinate system is rotated by $90-K_r$ about y axis and displaced to the lateral surface (x' and y' are placed on the lateral surface); $x''\ y''\ z''$ oblique coordinate system is obtained when $x'\ y'\ z'$ coordinate system is rotated by i (x'' placed on the lateral surface and oriented along the tool's cutting edge, y''also placed on the lateral surface, z'' normal to the lateral surface).

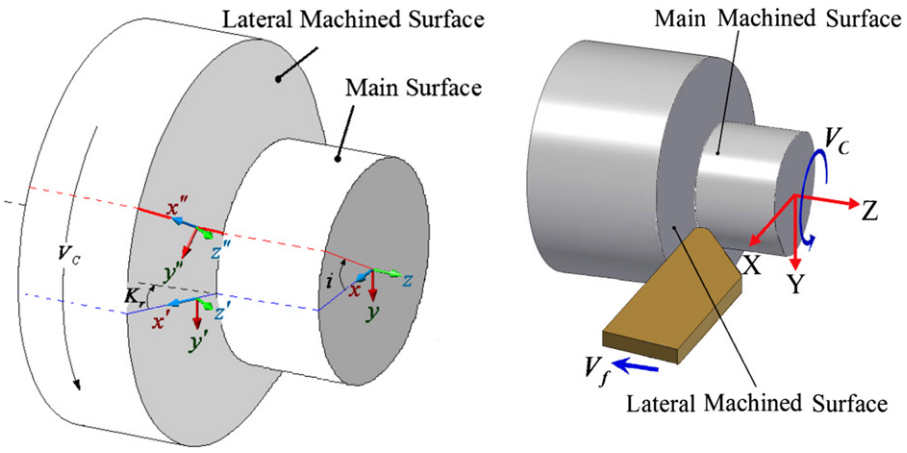

Fig. 1. A schematic view of oblique turning ($i \neq 0$,$K_r \leq 90^\circ$).

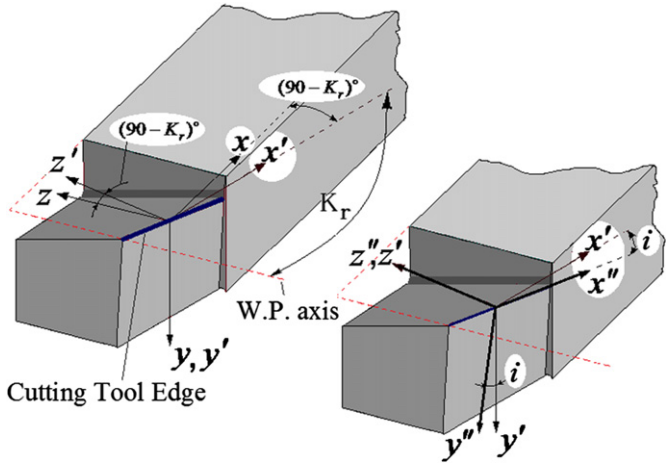

Fig. 2. Cutting tool in oblique turning ($i \neq 0$, $K_r \leq 90^\circ$).

The cutting tool in relation to the coordinate systems is shown in Fig. 2. It should be noted that the angles in oblique cutting follow the relation ($i \neq 0, K_r \leq 90^\circ$). The difference in the base points of the coordinate systems in Figs. 1 and 2 does not influence the results since the relative displacement, velocity and acceleration of the tool and workpiece are concerned.

A three dimensional view of the orthogonal and oblique 1D-UATs is illustrated in Fig. 3 where the vibration is applied along the cutting velocity. In this figure P_n denotes the normal plane (perpendicular to the tool cutting edge); V_f is the feed rate; V_C , the cutting speed; a and f, the vibration amplitude and frequency, respectively; and t, time.

The workpiece's velocity in 1D –UAT can be represented in $x\ y\ z$ system, as follows:

$$\vec{V}_W(t) = (V_{X_W}(t), V_{Y_W}(t), V_{Z_W}(t)) = (0, V_C, 0) \tag{1}$$

The cutting tool velocity in 1D-UAT can be written in $x\ y\ z$ system, as follows:

$$\vec{V}_T(t) = (V_{X_T}(t), V_{Y_T}(t), V_{Z_T}(t)) = (0, a\omega \sin \omega t, -V_f) \tag{2}$$

The workpiece's velocity relative to the cutting tool in UAT can thus be obtained as

$$\begin{aligned}\vec{V}_{W/T}(t) &= \vec{V}_W(t) - \vec{V}_T(t) = (V_{X_{W/T}}(t), V_{Y_{W/T}}(t), V_{Z_{W/T}}(t)) \\ &= (0, -a\omega \sin \omega t + V_C, V_f)\end{aligned} \tag{3}$$

where $V_{X_{W/T}}(t)$, $V_{Y_{W/T}}(t)$ and $V_{Z_{W/T}}(t)$ are the x, y and z components of velocity, respectively. The transformation from $x\ y\ z$ system to $x'\ y'\ z'$ system is done by the use of the following rotation matrix:

$$\begin{bmatrix} x' \\ y' \\ z' \end{bmatrix} = \begin{bmatrix} \cos(\pi/2 - K_r) & 0 & -\sin(\pi/2 - K_r) \\ 0 & 1 & 0 \\ \sin(\pi/2 - K_r) & 0 & \cos(\pi/2 - K_r) \end{bmatrix} \times \begin{bmatrix} x \\ y \\ z \end{bmatrix} \tag{4}$$

Consequently, it can be shown that the workpiece's velocity relative to the cutting tool in $x'\ y'\ z'$ coordinate system is obtained as

$$\begin{aligned}\vec{V}_{W/T}(t) &= \left(V_{X'_{W/T}}(t), V_{Y'_{W/T}}(t), V_{Z'_{W/T}}(t)\right) \\ &= (-\cos K_r V_f, -a\omega \sin \omega t + V_C, \sin K_r V_f)\end{aligned} \tag{5}$$

The $x'\ y'\ z'$ system is transformed to $x''\ y''\ z''$ system, as follows:

$$\begin{bmatrix} x'' \\ y'' \\ z'' \end{bmatrix} = \begin{bmatrix} \cos i & -\sin i & 0 \\ \sin i & \cos i & 0 \\ 0 & 0 & 1 \end{bmatrix} \times \begin{bmatrix} x' \\ y' \\ z' \end{bmatrix} \tag{6}$$

Therefore, the workpiece's position and speed relative to the cutting tool are obtained as follows:

$$\begin{aligned}X''_{W/T}(t) &= (\cos i) X'_{W/T}(t) + (-\sin i) Y'_{W/T}(t) \\ &= -a \sin i \cos \omega\, t - V_C \sin i\, t - \cos i \cos K_r V_f t\end{aligned} \tag{7}$$

$$\begin{aligned}Y''_{W/T}(t) &= (\sin i) X'_{W/T}(t) + (\cos i) Y'_{W/T}(t) \\ &= a \cos i \cos \omega t + V_C \cos it - \sin i \cos K_r V_f t\end{aligned} \tag{8}$$

$$Z''_{W/T}(t) = Z'_{W/T}(t) = \sin K_r V_f t \tag{9}$$

$$\begin{aligned}\vec{V}_{W/T}(t) &= (V_{X''_{W/T}}(t), V_{Y''_{W/T}}(t), V_{Z''_{W/T}}(t)) \\ &= \big(a\omega \sin i \sin \omega t - V_C \sin i - \cos i \cos K_r V_f, \\ &\quad -a\omega \cos i \sin \omega t + V_C \cos i \\ &\quad -\sin i \cos K_r V_f, \sin K_r V_f \big)\end{aligned} \tag{10}$$

3. Tool path

The tool path in UAT obtained by Eqs. 8 and 9 is illustrated in Fig. 4. It is more convenient to use a fixed workpiece system in which the cutting tool moves towards the workpiece. In this case ($Y''_{T/W}(t) = -Y''_{W/T}(t), Z''_{T/W}(t) = -Z''_{W/T}(t)$).

The tool path has been simulated by MATLAB software and illustrated in Fig. 5. This figure shows the first pass of UAT and the lateral surface left in P_n plane.

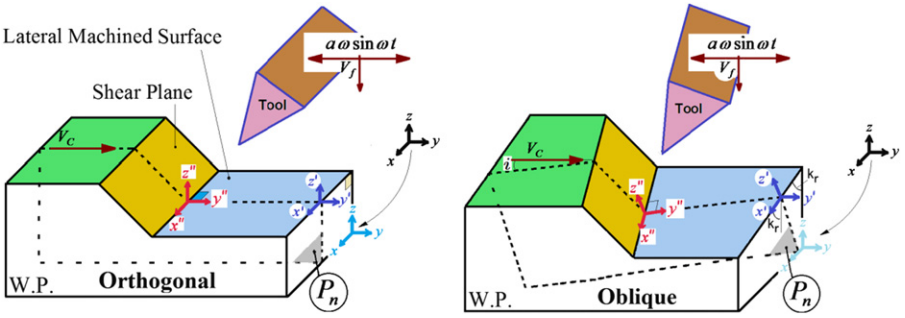

Fig. 3. A view of the orthogonal and oblique 1D-UATs.

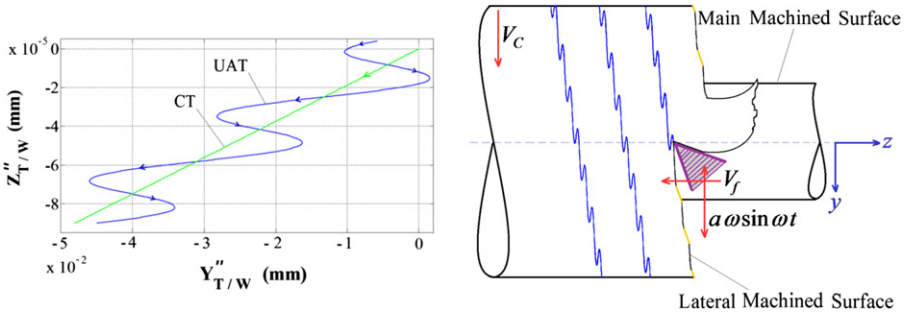

Fig. 4. The position of cutting tool edge relative to workpiece (V_f=0.4 mm/rev, V_C=0.36 m/s).

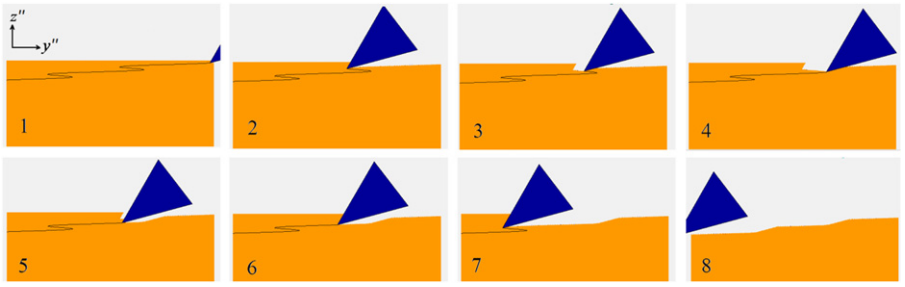

Fig. 5. 2D simulation of lateral surface in first pass of UAT; V_C=0.36 m/s, V_f=7.5 *mm/rev*, a=10 μm.

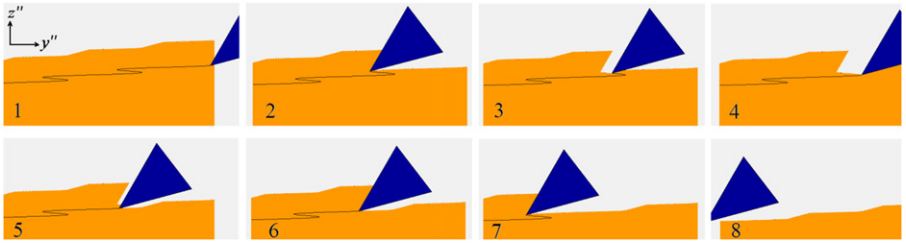

Fig. 6. a2D simulation of lateral surface in second pass of UAT; V_C=0.36 m/s, V_f=7.5 *mm/rev*, a=10 μm.

Similarly, the tool path and the lateral surface left in the second pass of UAT can be simulated as shown in Fig. 6.

An important point to note in Figs. 5 and 6 is that in order to present a clear illustration of the tool path, a feed rate about 50 times greater than its actual value has been selected, i.e. 7.5 mm/rev instead of 0.25 mm/rev. In conventional turning, the cutting tool moves along a straight path which can be simulated by an inclined line. In UAT, a toothed pattern is also superimposed on the inclined tool path, as can be seen in the simulation results shown in Figs. 5 and 6.

According to Figs. 5 and 6, the chip removal operation is carried out during stages 1–2. In stages 2–4, the cutting tool withdraws from the cutting zone causing the chip removal operation to stop. However, the cutting tool does not disengage in this stage from the workpiece because of its feed motion. It inevitably rubs and presses against the lateral surface. In stages 4–6, the cutting tool moves back toward the cutting zone and because of its feed motion, machines a very thin layer of the lateral surface under the assumption of sharp cutting edge. However, the feed component in z'' direction is usually smaller than the radius of the cutting tool edge due to the lack of sharpness. As a result, material removal in stages 4–6 is improbable and the surface is again rubbed by the cutting tool. In stages 6–8, chip removal from the uncut surface restarts.

In practice, it is expected that rubbing and pressing against the lateral surface to result in surface hardening. The pressed region

in each vibration cycle can be specified by its depth and width denoted by D and W, respectively, as illustrated in Fig. 7-a.

The surface hardness is measured by a micro-hardness device as described later in Part III. Several pressed and machined regions are covered by the device's indenter as shown in Fig. 7b. Therefore, the measured hardness represents an average value for the hardness of the pressed and machined regions. The indentation area on the lateral surface is simulated as shown in Fig. 8. The depths and widths of the pressed regions for different feed rates and cutting speeds are shown in this figure.

It is evident from Fig. 8 that when the feed rate is constant, the depth and width of the pressed region change with a change in the cutting speed V_C; by increasing the cutting speed, the width of the pressed region decreases ($W_1 > W_2 > W_3$), but its depth increases ($D_1 < D_2 < D_3$) (Fig. 8a). When the cutting speed V_C is constant, the width of the pressed region remains constant ($W_1 = W_2 = W_3$) but its depth increases ($D_1 < D_2 < D_3$)with an increase in the feed rate (Fig. 8b).

The effect of ultrasonic vibration amplitude on the width and depth of pressed regions is shown in Fig. 9. It can be seen from this figure that the depth of the pressed region remains constant but its width increases with an increase in the vibration amplitude.

An increase in the depth or width of the pressed region is expected to lead to the increase in the hardness of the lateral surface.

4. Critical speed in oblique UAT

The critical speed in vibration cutting denotes the maximum cutting speed as the threshold above which the cutting operation changes from the interrupted mode to continuous mode. In order to calculate the critical speed in oblique UAT, a proper criterion is required to distinguish between the engagement and disengagement of the cutting tool and workpiece. In the following sections three different criteria are proposed for this purpose and examined by case studies.

4.1. Critical speed: first criterion

The first criterion is explained with the aid of Fig. 10. This criterion implies that the cutting tool disengages from shear zone when the former leaves the plane normal to y'' axis at the chip root. This necessarily happens when the y'' component of the workpiece's velocity relative to the cutting tool becomes negative (Eq. 10). The y'' component of the relative velocity is denoted by $V_\perp$ in the first criterion. It should be noted that $V_\perp$ is an auxiliary parameter which is differently defined for the three criteria.

The y'' component of relative velocity is rewritten from Eq. (10), as follows:

$$V_\perp = V_{Y'_{W/T}}(t) = -a\omega \cos i \sin \omega t + V_C \cos i - \sin i \cos K_r V_f \qquad (11)$$

Similar to orthogonal UAT, the critical speed can be inferred as the threshold over which the speed of ultrasonic vibration

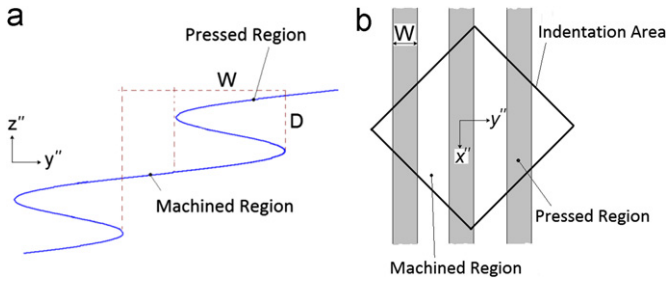

Fig. 7. A view of (a) the width and depth of pressed region in one vibration cycle, (b) the indentation area.

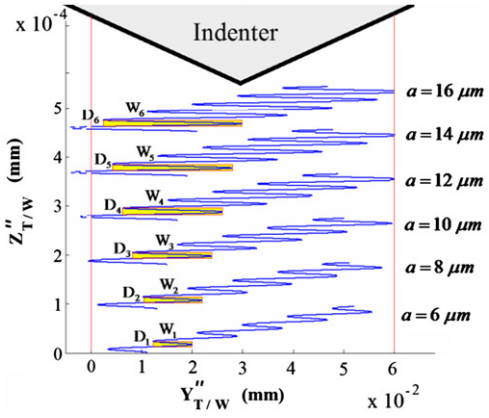

Fig. 9. The effect of ultrasonic vibration amplitude on the width and depth of pressed regions; V_C=0.18 m/s, V_f=0.4 mm/rev, f=20 kHz, $D_1=D_2=D_3=D_4=D_5=D_6$, $W_1 < W_2 < W_3 < W_4 < W_5 < W_6$.

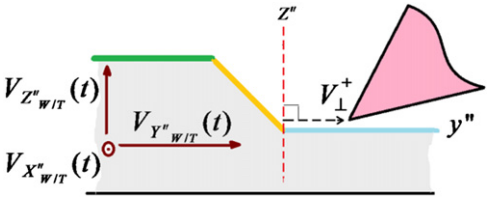

Fig. 10. Illustration of the first criterion.

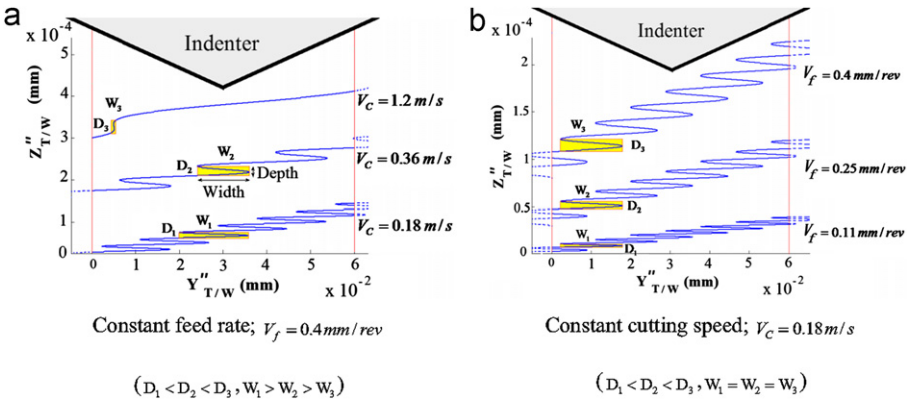

Fig. 8. The effect of different machining parameters on depth and width of pressed regions.

approaches the cutting speed. This threshold for oblique UAT can be obtained by setting Eq. 11 to zero. The first derivative of $V_\perp$ would be zero at critical speed since $V_\perp$ attains its minimum:

$$dV_\perp/dt = -a\omega^2 \cos i \cos \omega t = 0 \Rightarrow \cos \omega = 0 \Rightarrow \sin \omega t = \pm 1 \quad (12)$$

$$d^2V_\perp/dt^2 = +a\omega^3 \cos i \sin \omega\, t > 0 \Rightarrow \sin \omega t > 0 \Rightarrow \sin \omega t = +1 \quad (13)$$

By substituting $\sin \omega\, t = +1$ in Eq. 11 and setting this equation to zero, the critical speed is obtained as follows:

$$V_{cr} = +a\,\omega + \cos K_r \tan i V_f (m/s) \quad (14)$$

In turning process, the feed rate V_f (mm/rev) and cutting speed are related to each other, as follows: $V_f\,(m/s) = (V_f\,(\text{mm/rev}) \times V_C\,(m/s))/(\pi d\,(\text{mm}))$. At the critical speed, $V_C$in this relation is substituted by V_{cr}. By substituting V_f from this relation into Eq. (14), the critical speed can be rewritten as follows:

$$V_{cr} = \frac{\pi da\omega}{\pi d - \cos K_r \tan i V_f\,(\text{mm/rev})} \quad (15)$$

4.2. Critical speed: second criterion

The second criterion is explained with the aid Fig. 11. This criterion implies that the cutting tool disengages from the shear zone when the tool's rake face disengages from chip.

The relative velocity $V_\perp$, is written as follows (Fig. 11 and Eq. (10)):

$$V_\perp = (\cos \gamma_n) V_{Y'_{W/T}}(t) + (-\sin \gamma_n) V_{Z'_{W/T}}(t) = [-a\omega \cos i \sin \omega t + V_C \cos i - \sin i \cos K_r V_f] \cos \gamma_n - [\sin K_r V_f] \sin \gamma_n \quad (16)$$

where γ_n is the normal 3rake angle. The critical speed for the second criterion is obtained in a way similar to the first criterion, as follows:

$$V_{cr} = +a\omega + \left(\frac{\sin K_r \tan \gamma_n}{\cos i} + \cos K_r \tan i\right) V_f\,(m/s) \quad (17)$$

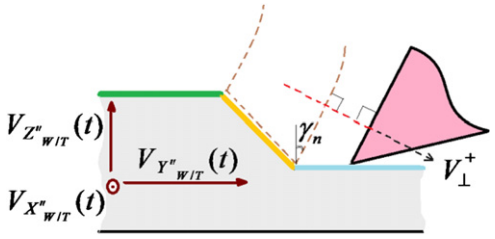

Fig. 11. Illustration of the second criterion.

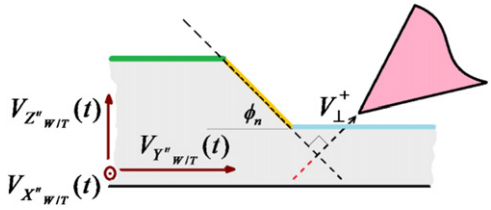

Fig. 12. Illustration of the third criterion.

or

$$V_{cr} = \frac{\pi da\omega}{\pi d - ((\sin K_r \tan \gamma_n/\cos i) + \cos K_r \tan i) V_f\,(\text{mm/rev})} \quad (18)$$

4.3. Critical speed: third criterion

The third criterion is explained with the aid of Fig. 12. This criterion implies that the cutting tool disengages from the shear zone when the tool's cutting edge disengages from the shear plane.

The relative velocity $V_\perp$, is written as (Fig. 12 and Eq. (10)):

$$V_\perp = (\sin \phi_n) V_{Y'_{W/T}}(t) + (\cos \phi_n) V_{Z'_{W/T}}(t) = [-a\omega \cos i \sin \omega t + V_C \cos i - \sin i \cos K_r V_f] \sin \phi_n + [\sin K_r V_f] \cos \phi_n \quad (19)$$

where ϕ_n is the normal shear angle. The critical speed for the third criterion can be found, as follows:

$$V_{cr} = +a\omega + \left(\cos K_r \tan i - \frac{\sin K_r \cot \phi_n}{\cos i}\right) V_f\,(m/s) \quad (20)$$

or

$$V_{cr} = \frac{\pi da\omega}{\pi d - (\cos K_r \tan i - (\sin K_r \cot \phi_n/\cos i)) V_f\,(\text{mm/rev})} \quad (21)$$

The normal shear angle φ_n in UAT is time dependent and changes during cutting operation. The important point is that the values of the normal shear angle at the engagement and disengagement moments are the same in each cycle of vibration.

5. Cutting and noncutting duration in oblique UAT

Three criteria were proposed in previous section for distinguishing the disengagement instant of the cutting tool from the shear zone. Accordingly, three criteria can also be presented to find out the reengagement instant of the cutting tool. These criteria are schematically depicted with the aid of Fig. 13. In this figure, $t_{1\ 1}$ and $t_{1\ 3}$ are the disengagement and reengagement instants of the cutting tool or, in other words, the machining interruption and restart instants, respectively.

The tool path relative to the workpiece can be drawn in the normal plane by using Eqs. (8) and (9), as depicted in Fig. 14. In this figure, $t_{1\ 2}$ denotes the instant of maximum distance of the cutting tool from the shear zone. The points $t_{1\ 1}$, $t_{1\ 2}$, $t_{1\ 3}$ are related to the first and $t_{n\ 1}$, $t_{n\ 2}$, $t_{n\ 3}$ to the nth vibration cycle. The spring back of chip and workpiece has been neglected.

As is evident from the nature of UAT process, the cutting operation is performed in part of each vibration cycle. The intention in this section is to develop analytical means for prediction of the cutting and noncutting duration in each cycle of vibration. The engagement and disengagement instants in consecutive vibration cycles can be used to derive the cutting and noncutting duration. Different relations are necessarily obtained in terms of the above mentioned criteria, as follows.

5.1. Cutting and noncutting duration: first criterion

The machining interruption and restart instants, i.e. $t_{1\ 1}$ and $t_{1\ 3}$, are illustrated in Fig. 15 for the first criterion.

The machining interruption instant, $t_{1\ 1}$, is obtained by setting $V_\perp$ from Eq. (11) to zero, as follows:

$$V_\perp = V_{Y'_{W/T}}(t) = -a\omega \cos i \sin \omega t + V_C \cos i - \sin i \cos K_r V_f = 0 \Rightarrow \sin \omega t = \frac{V_C \cos i - V_f \sin i \cos K_r}{2\pi a f \cos i}$$

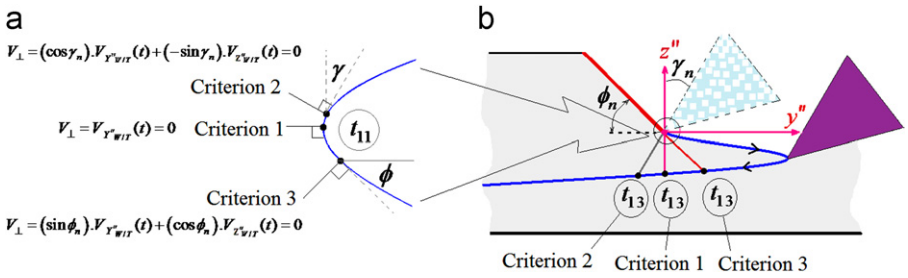

Fig. 13. Illustration of three criteria for (a) disengagement instant $t_{1\,1}$ and (b) reengagement instant $t_{1\,3}$ of the cutting tool.

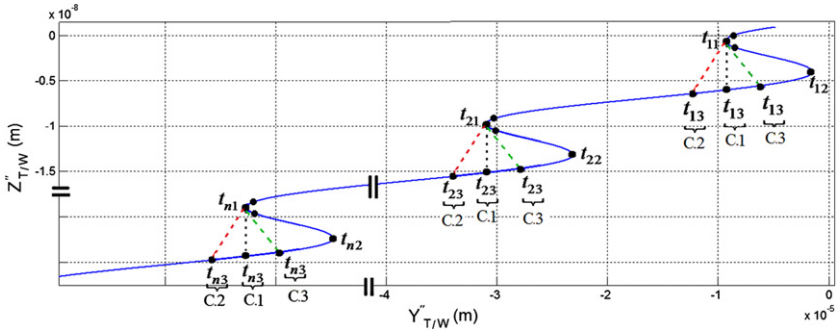

Fig. 14. The tool path relative to workpiece in UAT; C1, C2, C3 implying 1st, 2nd, 3rd criteria; $i=30^\circ$, $K_r=60^\circ$, $\gamma_n=30^\circ$, V_C=0.5 m/s, a=10 μm and V_f=0.2 mm/rev.

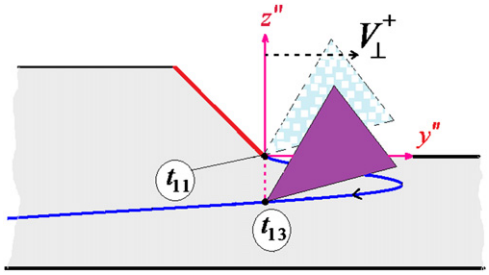

Fig. 15. Disengagement and reengagement of cutting tool according to the 1st criterion.

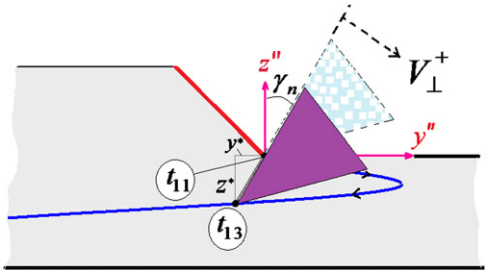

Fig. 16. Disengagement and reengagement of cutting tool according to the 2nd criterion.

$$\Rightarrow \begin{cases} \omega t+2K\pi=\sin^{-1}\left(\frac{V_C\cos i-V_f\sin i\cos K_r}{2\pi a f\cos i}\right) \\ \pi-\omega t+2K\pi=\sin^{-1}\left(\frac{V_C\cos i-V_f\sin i\cos K_r}{2\pi a f\cos i}\right) \end{cases} \quad (22)$$

The general roots of the above equations are calculated as follows:

$$t_{n1}=\frac{\sin^{-1}(V_C\cos i-V_f\sin i\cos K_r/2\pi a f\cos i)}{2\pi f}+\frac{n-1}{f} \quad (23)$$

$$t_{n2}=\frac{1}{2f}-\frac{\sin^{-1}(V_C\cos i-V_f\sin i\cos K_r/2\pi a f\cos i)}{2\pi f}+\frac{n-1}{f} \quad (24)$$

where n is the number of vibration cycle. For the first cycle:

$$t_{1\,1}=\frac{\sin^{-1}(V_C\cos i-V_f\sin i\cos K_r/2\pi a f\cos i)}{2\pi f} \quad (25)$$

$$t_{12}=\frac{1}{2f}-\frac{\sin^{-1}(V_C\cos i-V_f\sin i\cos K_r/2\pi a f\cos i)}{2\pi f} \quad (26)$$

It is sensible to assume that the machining operation restarts when the cutting tool returns back to its $t_{1\,1}$ position relative to the workpiece along y''axis (Fig. 15). Therefore, $t_{1\,3}$ can be estimated as follows:

$$Y''_{W/T}(t_{1\,1})=Y''_{W/T}(t_{1\,3}) \quad (27)$$

By substituting from Eq. (8) into the above equation:

$$a\cos i\cos\omega t_{11}+V_C\cos it_{11}-\sin i\cos K_rV_ft_{11}=a\cos i\cos\omega t_{13}+V_C\cos it_{13}-\sin i\cos K_rV_ft_{13} \quad (28)$$

The only unknown parameter in the above equations is $t_{1\,3}$, so the equation can be written in the form of $A\cos Bt_{13}+Ct_{13}=D$ (A, B, C and D as computable constants). This equation has no analytical solution and should be solved numerically within the specified time interval $t_{1\,2}$ to $t_{2\,1}$.

5.2. Cutting and noncutting duration: second criterion

The machining interruption and restart instants, i.e. $t_{1\,1}$ and $t_{1\,3}$, are illustrated in Fig. 16 for the second criterion.

The machining interruption instant, $t_{1\,1}$, is obtained by setting $V_\perp$ from Eq. (16) to zero, as follows:

$$V_\perp=(-a\omega\cos i\sin\omega t+V_C\cos i-\sin i\cos K_rV_f)\cos\gamma_n-(\sin K_rV_f)\sin\gamma_n=0$$

$$\Rightarrow \sin\omega t=\frac{V_C\cos i-V_f(\sin i\cos K_r+\tan\gamma_n\sin K_r)}{2\pi a f\cos i} \quad (29)$$

The general roots of the above equations are calculated as follows:

$$t_{n1}=\frac{\sin^{-1}(V_C\cos i-V_f(\sin i\cos K_r+\tan\gamma_n\sin K_r)/2\pi af\cos i)}{2\pi f}+\frac{n-1}{f} \tag{30}$$

$$t_{n2}=\frac{1}{2f}-\frac{\sin^{-1}(V_C\cos i-V_f(\sin i\cos K_r+\tan\gamma_n\sin K_r)/2\pi af\cos i)}{2\pi f}+\frac{n-1}{f} \tag{31}$$

According to Fig. 16, the machining restart instant, t_{13}, is obtained as follows:

$$\begin{cases} Y''_{W/T}(t_{11})+Y^*=Y''_{W/T}(t_{13}) \\ Z''_{W/T}(t_{11})+Z^*=Z''_{W/T}(t_{13}) \end{cases}$$

$$V_{Z''_{W/T(mean)}}(t)=\frac{Z''_{W/T}(t_{13})-Z''_{W/T}(t_{11})}{t_{13}-t_{11}}=\frac{Z^*}{t_{13}-t_{11}}\Rightarrow Z^*=V_{Z'_{W/T(mean)}}(t)\times(t_{13}-t_{11})$$

$$\tan\gamma_n=\frac{Y^*}{Z^*}\quad\Rightarrow$$

$$Y''_{W/T}(t_{13})-Y''_{W/T}(t_{11})=Y^*=\tan\gamma_n Z^*=\tan\gamma_n V_{Z'_{W/T(mean)}}(t)\times(t_{13}-t_{11}) \tag{32}$$

By substituting from Eqs. (8) and (10) into the above equation:

$$a\cos i\cos\omega t_{13}+V_C\cos i t_{13}-\sin i\cos K_r V_f t_{13}-a\cos i\cos\omega t_{11}-V_C\cos i t_{11}+\sin i\cos K_r V_f t_{11}=\tan\gamma_n\sin K_r V_f\ (t_{13}-t_{11}) \tag{33}$$

The above equation can be solved numerically to obtain the only unknown parameter, t_{13}, within the time interval t_{12} to t_{21}.

5.3. Cutting and noncutting duration: third criterion

The machining interruption and restart instants, i.e. t_{11} and t_{13}, are illustrated in Fig. 17 for the third criterion.

The machining interruption instant, t_{11}, is obtained by setting $V_\perp$ from Eq. (19) to zero, as follows:

$$V_\perp=[-a\omega\cos i\sin\omega t+V_C\cos i-\sin i\cos K_r V_f]\sin\phi_n+[\sin K_r V_f]\cos\phi_n=0$$

$$\Rightarrow\quad \sin\omega t=\frac{V_C\cos i-V_f\ (\sin i\cos K_r-\cot\phi_n\sin K_r)}{2\pi a f\cos i} \tag{34}$$

The general roots of the above equations are calculated as follows:

$$t_{n1}=\frac{\sin^{-1}(V_C\cos i-V_f(\sin i\cos K_r-\cot\phi_n\sin K_r)/2\pi af\cos i)}{2\pi f}+\frac{n-1}{f} \tag{35}$$

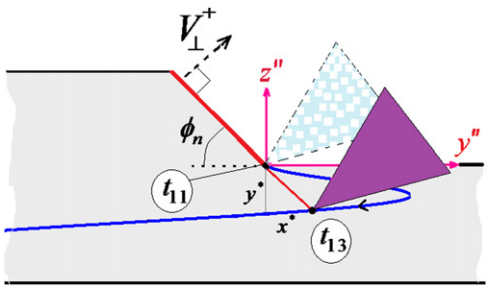

Fig. 17. Disengagement and reengagement of cutting tool according to the 3rd criterion.

$$t_{n2}=\frac{1}{2f}-\frac{\sin^{-1}(V_C\cos i-V_f(\sin i\cos K_r-\cot\phi_n\sin K_r)/2\pi af\cos i)}{2\pi f}+\frac{n-1}{f} \tag{36}$$

According to Fig. 17, the machining restart instant, t_{13}, is obtained as follows:

$$\begin{cases} Y''_{W/T}(t_{11})-Y^*=Y''_{W/T}(t_{13}) \\ Z''_{W/T}(t_{11})+Z^*=Z''_{W/T}(t_{13}) \end{cases}$$

$$V_{Z'_{W/T}}(t)=\frac{Z^*}{t_{13}-t_{11}}\Rightarrow Z^*=V_{Z'_{W/T}}(t)\times(t_{13}-t_{11})$$

$$\cot\phi_n=\frac{Y^*}{Z^*}\Rightarrow$$

$$Y^*=Y''_{W/T}(t_{11})-Y''_{W/T}(t_{13})=\cot\phi_n Z^*=\cot\phi_n V_{Z'_{W/T}}(t)\times(t_{13}-t_{11}) \tag{37}$$

By substituting from Eqs. (8) and (10) into the above equation:

$$a\cos i\cos\omega t_{11}+V_C\cos i t_{11}-\sin i\cos K_r V_f t_{11}-a\cos i\cos\omega t_{13}-V_C\cos i t_{13}+\sin i\cos K_r V_f t_{13}=\cot\phi_n\sin K_r V_f(t_{13}-t_{11}) \tag{38}$$

The above equation can be solved numerically to obtain the only unknown parameter, t_{13}, within the time interval t_{12} to t_{21}.

5.4. Case studies

Several examples are presented in this section for different values of vibration amplitude and cutting speed to examine the criteria discussed above. The other oblique UAT parameters are assumed to be as follows: vibration frequency $f=20$ kHz; feed rate $V_f=0.2$ mm/rev; workpiece diameter $d=150$ mm; and the angles of inclination, tool cutting edge and normal rake $i=30^\circ$, $K_r=60^\circ$ *and* $\gamma_n=30^\circ$, respectively. The times t_{11}, t_{12} and t_{13} can be calculated from Eqs. (23), (24) and (28) for the first criterion; Eqs. (30), (31) and (33) for the second criterion; and Eqs. (35), (36) and (38) for the third criterion, respectively. As mentioned earlier, t_{13} is calculated numerically within the time interval (t_{12} to t_{21}). The numerical solutions have been obtained by MATLAB software. The following definitions hold for the examples presented in this section: vibration cycle time $\Delta t_{total}=t_{21}-t_{11}=1/f$, noncutting duration in one cycle of vibration $\Delta t_1=t_{13}-t_{11}$, cutting duration in a cycle of vibration $\Delta t_2=t_{21}-t_{13}$, the ratio of cutting duration to cycle time $\Delta t_2/\Delta t_{total}$. The results of calculation are presented in Tables 1–3 for criteria 1–3, respectively.

As can be seen in Tables 1–3, $\Delta t_1=0$ for cases 2, 3 and 5. That means no cutting interruption occurs and the cutting tool is continuously engaged with the workpiece in these examples.

6. Results and discussion

The machining interruption and restart instants for the three criteria are compared in Fig. 18a (for case 1) and Fig. 18b (for case 4).

The ratios of cutting duration to total cycle time, $\Delta t_2/\Delta t_{\text{total}}$, obtained for the three criteria are shown in Fig. 19.

As can be seen in Fig. 19, the minimum value of $\Delta t_2/\Delta t_{total}$ is obtained for the second criterion. This ratio is higher in the third criterion compared with two others.

The average of $\Delta t_2/\Delta t_{total}$ obtained for the three criteria for different cutting velocities and vibration amplitudes are shown in Fig. 20. It is evident from this figure that an increase in the vibration amplitude and decrease in the cutting speed result in a lower$\Delta t_2/\Delta t_{total}$ indicating that the ultrasonic vibration will be more effective.

Table 1
The results of examples for the 1st criterion; $i=30^{\circ}$, $K_r=60^{\circ}$, $\gamma_n=30^{\circ}$, $V_f=0.2$ mm/rev, $d=150\,mm$.

		t_{11}	t_{12}	t_{13}	t_{21}	Δt_{total}	Δt_1	Δt_2	$\Delta t_2/\Delta t_{total}$
1	$a=6\,\mu m$ $V_C=0.5\,m/s$	5.7703×10^{-6}	1.9230×10^{-5}	2.65282×10^{-5}	5.5770×10^{-5}	5×10^{-5}	2.07579×10^{-5}	2.92418×10^{-5}	0.584836
2	$a=6\,\mu m$ $V_C=0.754\,m/s$	1.25×10^{-5}	1.25×10^{-5}	1.25×10^{-5}	6.25×10^{-5}	5×10^{-5}	0	5×10^{-5}	1
3	$a=6\,\mu m$ $V_C=1.7\,m/s$	1.25×10^{-5}	1.25×10^{-5}	1.25×10^{-5}	6.25×10^{-5}	5×10^{-5}	0	5×10^{-5}	1
4	$a=10\,\mu m$ $V_C=0.5\,m/s$	3.2568×10^{-6}	2.1743×10^{-5}	3.27802×10^{-5}	5.3257×10^{-5}	5×10^{-5}	2.95234×10^{-5}	2.04768×10^{-5}	0.409536
5	$a=10\,\mu m$ $V_C=1.7\,m/s$	1.25×10^{-5}	1.25×10^{-5}	1.25×10^{-5}	6.25×10^{-5}	5×10^{-5}	0	5×10^{-5}	1

Table 2
The results of examples for the 2nd criterion; $i=30^{\circ}$, $K_r=60^{\circ}$, $\gamma_n=30^{\circ}$, $V_f=0.2$ mm/rev, $d=150\,mm$.

		t_{11}	t_{12}	t_{13}	t_{21}	Δt_{total}	Δt_1	Δt_2	$\Delta t_2/\Delta t_{total}$
1	$a=6\,\mu m$ $V_C=0.5\,m/s$	5.7686×10^{-6}	1.9231×10^{-5}	2.65322×10^{-5}	5.5769×10^{-5}	5×10^{-5}	2.07636×10^{-5}	2.9236×10^{-5}	0.58473
2	$a=6\,\mu m$ $V_C=0.754\,m/s$	1.25×10^{-5}	1.25×10^{-5}	1.25×10^{-5}	6.25×10^{-5}	5×10^{-5}	0	5×10^{-5}	1
3	$a=6\,\mu m$ $V_C=1.7\,m/s$	1.25×10^{-5}	1.25×10^{-5}	1.25×10^{-5}	6.25×10^{-5}	5×10^{-5}	0	5×10^{-5}	1
4	$a=10\,\mu m$ $V_C=0.5\,m/s$	3.2560×10^{-6}	2.1744×10^{-5}	3.27826×10^{-5}	5.3256×10^{-5}	5×10^{-5}	2.95266×10^{-5}	2.04734×10^{-5}	0.40947
5	$a=10\,\mu m$ $V_C=1.7\,m/s$	1.25×10^{-5}	1.25×10^{-5}	1.25×10^{-5}	6.25×10^{-5}	5×10^{-5}	0	5×10^{-5}	1

Table 3
The results of examples for the 3rd criterion; $i=30^{\circ}$, $K_r=60^{\circ}$, $\gamma_n=30^{\circ}$, $V_f=0.2$ mm/rev, $d=150\,mm$.

		t_{11}	t_{12}	t_{13}	t_{21}	Δt_{total}	Δt_1	Δt_2	$\Delta t_2/\Delta t_{total}$
1	$a=6\,\mu m$ $V_C=0.5\,m/s$	5.7733×10^{-6}	1.9227×10^{-5}	2.65214×10^{-5}	5.5773×10^{-5}	5×10^{-5}	2.07481×10^{-5}	2.92516×10^{-5}	0.585032
2	$a=6\,\mu m$ $V_C=0.754\,m/s$	1.25×10^{-5}	1.25×10^{-5}	1.25×10^{-5}	6.25×10^{-5}	5×10^{-5}	0	5×10^{-5}	1
3	$a=6\,\mu m$ $V_C=1.7\,m/s$	1.25×10^{-5}	1.25×10^{-5}	1.25×10^{-5}	6.25×10^{-5}	5×10^{-5}	0	5×10^{-5}	1
4	$a=10\,\mu m$ $V_C=0.5\,m/s$	3.2583×10^{-6}	2.17417×10^{-5}	3.27762×10^{-5}	5.32583×10^{-5}	5×10^{-5}	2.95179×10^{-5}	2.04821×10^{-5}	0.409642
5	$a=10\,\mu m$ $V_C=1.7\,m/s$	1.25×10^{-5}	1.25×10^{-5}	1.25×10^{-5}	6.25×10^{-5}	5×10^{-5}	0	5×10^{-5}	1

A smaller ratio of the cutting duration to the cycle time, $\Delta t_2/\Delta t_{total}$, indicates that for a specific cycle time, the duration of the cutting tool engagement with the workpiece is less than that in the larger values of $\Delta t_2/\Delta t_{total}$. This phenomenon leads to lower average cutting force and thus to the higher effectiveness of ultrasonic vibration cutting.

If the feed rate is neglected the critical speeds in oblique UAT obtained for the three criteria will converge to ($V_{cr}=2\,\pi\,a\,f$)

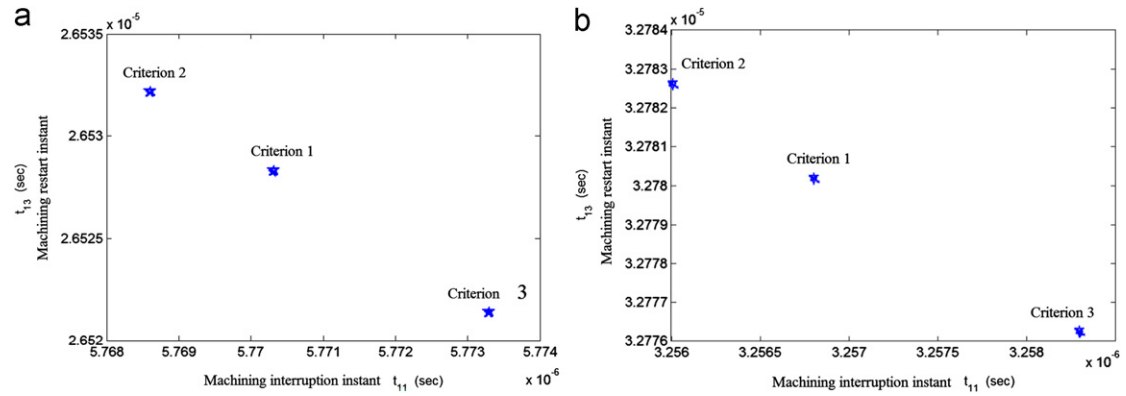

Fig. 18. Comparison of t_{11} and t_{13} for three criteria, (a) $a=6\ \mu m$, (b) $a=10\ \mu m$; $i=30^{\circ}$, $K_r=60^{\circ}$, $\gamma_n=30^{\circ}$, $V_C=0.5$ m/s, $V_f=0.2$ mm/rev, $d=150$ mm.

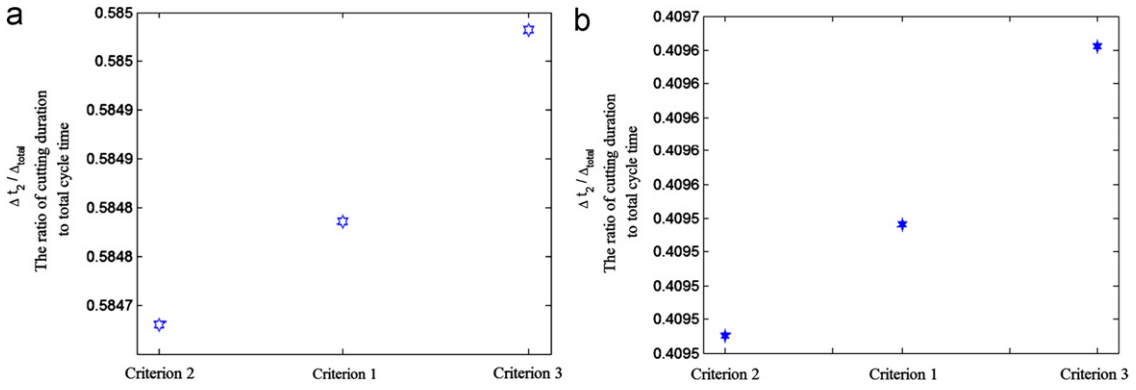

Fig. 19. The ratio of cutting duration to cycle time for three criteria, (a) $a=6\ \mu m$, (b) $a=10\ \mu m$; $i=30^{\circ}$, $K_r=60^{\circ}$, $\gamma_n=30^{\circ}$, $V_C=0.5$ m/s, $V_f=0.2$ mm/rev, $d=150$ mm.

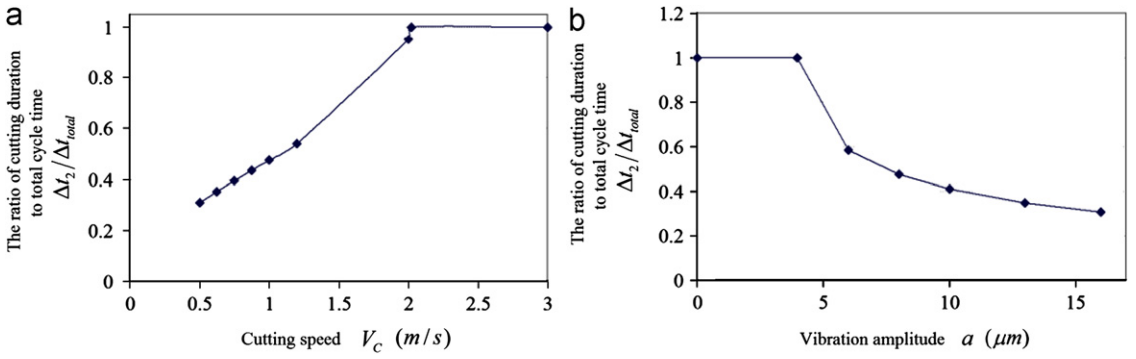

Fig. 20. The average of $\Delta t_2/\Delta t_{total}$ obtained for the three criteria, (a) versus V_C, (b) versus a; $i=30^{\circ}$, $K_r=60^{\circ}$, $\gamma_n=30^{\circ}$, $V_C=0.5$ m/s, $V_f=0.2$ mm/rev, $d=150$ mm.

which is the same as in orthogonal UAT. This can be verified by substituting $V_f=0$ in Eqs. (14), (15), (17), (18), (20) and (21). In that case, same value is obtained for each of $t_{1\ 1}$ and $t_{1\ 2}$ in the three criteria. This can be verified by substituting $V_f=0$ in Eqs. (25), (26), (30), (31), (35) and (36) which yields $t_{11}=\sin^{-1}(V_C/2\pi af)/2\pi f$ and $t_{12}=(1/2f)-\sin^{-1}(V_C/2\pi af)/2\pi f$.

As is expected, different estimates will be obtained for the machining interruption and restart instants for the three criteria if the feed rate is taken into consideration ($V_f\neq 0$). However, this difference is insignificant compared with the cycle time; it can be shown that the difference is in the order of 10^{-7} s whereas the cycle time is $\Delta t_{total}=5\times 10^{-5}$ s. The difference between $\Delta t_2/\Delta t_{total}$ s obtainable for the three criteria is about 0.002–0.003. This implies that any of the three criteria can viably be employed.

It should be noted that in the case of $V_C\geq V_{cr}$, the ratio of $\Delta t_2/\Delta t_{total}$ becomes 1. This means that the cutting tool continuously engages with the workpiece and the cutting operation is carried out during the whole cycle time (as can be seen in Fig. 20a, when V_C is greater than about 2 m/s and in Fig. 20-b when amplitude is less than about 4 μm). In case of $V_C<V_{cr}$, the cutting operation is intermittent and the advantages of applying ultrasonic vibration to the cutting tool will be maintained.

7. Conclusion

A kinematics model has been developed in the present study for the relative movement between the cutting tool and workpiece in UAT.

The model predicts that the cutting tool does not disengage from the workpiece during its cyclic motion and inevitably rubs and presses against the lateral surface remaining after each revolution of the workpiece. The tool path is the resultant of cutting motion, feed motion and ultrasonic vibration along the direction of the cutting velocity. This tool path leaves a toothed pattern on the lateral surface consisting of alternate pressed and machined regions. The pressed regions harden due to the burnishing effect. The model predicts that the width of pressed regions increases when the cutting speed decreases or the vibration amplitude increases; also an increase in the feed rate results in the increase of the depth of pressed regions which in turn may lead to increased hardness of the lateral surface. The kinematics model predicts no pressing on the lateral surface in UAT at higher cutting speeds. This agrees with the common understanding of UAT as the latter loses its advantages and performs like a CT process when the cutting speed approaches its critical value.

The critical speed and machining duration in each vibration cycle were other subjects dealt with in the present paper.

Three criteria were proposed to elaborate on the underlying mechanism of the machining interruption and restart in each vibration cycle for 1D-oblique UAT. If the feed rate is neglected the critical velocities in oblique UAT obtained for the three criteria will converge to $(V_{cr}=2\pi a\ f)$ which is the same as in orthogonal UAT. In that case the estimates of the criteria for the machining duration are also the same. The estimates of the criteria would of course be different when the feed rate is taken into consideration, but the difference is about $0.002-0.003$ for $\Delta t_2/\Delta t_{total}$ which is practically insignificant. Therefore, the three criteria proposed in the present study can equivalently be inferred as the underlying mechanism of the machining interruption and restart in each vibration cycle in 1D-oblique UAT.

It was found that by reducing the cutting speed or by increasing the vibration amplitude, the ratio of the cutting duration to the cycle time would decrease indicating that the ultrasonic vibration would be more effective at lower cutting speeds and larger vibration amplitudes.

References

[1] Shamoto Chunxiang Ma, E, Moriwaki T, Wang Lijiang. Study of machining accuracy in ultrasonic elliptical vibration cutting. Int J Mach Tool Manuf 2004;44:1305–10.

[2] Shamoto Chunxiang Ma, E, Moriwaki T, Zhang Yonghong, Wang Lijiang. Suppression of burrs in turning with ultrasonic elliptical vibration cutting. Int J Mach Tool Manuf 2005;45:1295–300.

[3] Nath C, Rahman M, Neo KS. A study on ultrasonic elliptical vibration cutting of tungsten carbide. J Mater Process Technol 2009;209:4459–64.

[4] Nath Chandra, Rahman Mustafizur, Soon Neo Ken. Machinability study of tungsten carbide using PCD tools under ultrasonic elliptical vibration cutting. Int J Mach Tool Manuf 2009;49:1089–95.

[5] Xiao M, Karube S, Soutome T, Sato K. Analysis of chatter suppression in vibration cutting. Int J Mach Tool Manuf 2002;42:1677–85.

[6] Xiao M, Wang QM, Sato K, Karube S, Soutome T, Xu H. The effect of tool geometry on regenerative instability in ultrasonic vibration cutting. Int J Mach Tool Manuf 2006;46:492–9.

[7] Nath Chandra, Rahman M, Andrew SSK. A study on ultrasonic vibration cutting of low alloy steel. J Mater Process Technol 2007;192-193:159–65.

[8] Nath Chandra, Rahman M. Effect of machining parameters in ultrasonic vibration cutting. Int J Mach Tool Manuf 2008;48:965–74.

[9] Rimkevičienė J, Ostaševičius V, Jūrėnas V, Gaidys R. Experiments and simulations of ultrasonically assisted turning tool. Mechanika 2009;75:42–6.

[10] Amini S, Soleimanimehr H, Nategh MJ, Abudollah A, Sadeghi MH. FEM analysis of ultrasonic-vibration-assisted turning and the vibratory tool. J Mater Process Technol 2008;201:43–7.

[11] Ahmed N, Mitrofanov AV, Babitsky VI, Silberschmidt VV. Analysis of material response to ultrasonic vibration loading in turning Inconel 718. Mater Sci Eng, A 2006;424:318–25.

[12] Ahmed N, Mitrofanov AV, Babitsky VI, Silberschmidt VV. Analysis of forces in ultrasonically assisted turning. J Sound Vib 2007;308:845–54.

[13] Harada Kei, Sasahara Hiroyuki. Effect of dynamic response and displacement/stress amplitude on ultrasonic vibration cutting. J Mater Process Technol 2009;209:4490–5.

[14] Mitrofanov AV, Babitsky VI, Silberschmidt VV. Finite element simulations of ultrasonically assisted turning. Comput Mater Sci 2003;28:645–53.

[15] Mitrofanov AV, Babitsky VI, Silberschmidt VV. Finite element analysis of ultrasonically assisted turning of Inconel 718. J Mater Process Technol 2004;153–154:233–9.

[16] Babitsky VI, Mitrofanov AV, Silberschmidt VV. Ultrasonically assisted turning of aviation materials: simulations and experimental study. Ultrasonics 2004;42:81–6.

[17] Mitrofanov AV, Ahmed N, Babitsky VI, Silberschmidt VV. Effect of lubrication and cutting parameters on ultrasonically assisted turning of Inconel 718. J Mater Process Technol 2005;162-163:649–54.

[18] Mitrofanov AV, Babitsky VI, Silberschmidt VV. Thermomechanical finite element simulations of ultrasonically assisted turning. Comput Mater Sci 2005;32:463–71.

[19] Ahmed N, Mitrofanov AV, Babitsky VI, Silberschmidt VV. 3D finite element analysis of ultrasonically assisted turning. Comput Mater Sci 2007;39:149–54.

[20] Kim Jeong-Du, Choi In-Hyu. Characteristics of chip generation by ultrasonic vibration cutting with extremely low cutting velocity. Int J Adv Manuf Technol 1998;14:2–6.

[21] Overcash Jerald L, Cuttino James F. In-process modeling of dynamic tool-tip temperatures of a tunable vibration turning device operating at ultrasonic frequencies. Precis Eng 2009;33:505–15.

[22] Sasahara Hiroyuki. The effect on fatigue life of residual stress and surface hardness resulting from different cutting conditions of 0.45%C steel. Int J Mach Tool Manuf 2005;45:131–6.

[23] J. Kumabe, Vibratory cutting. Tokyo: Jikkyou Publishing Co.,; 1979 [in Japanese].

[24] Astashev VK, Babitsky VI. Ultrasonic cutting as a nonlinear (vibro-impact) process. Ultrasonics 1998;36:89–96.

[25] Jin Masahiko, Murakawa Masao. Development of practical ultrasonic vibration cutting tool system. J Mater Process Technol 2001;113:342–7.